

Fig. 1. Stimulus waveform [see (4)].

This is zero for  $t < 0$ , of course, and may jump at  $t = 0$  depending on the discontinuity in  $I$  and the structure of  $G$ . For  $t > 0$  ( $\cong t'$ ) we assume  $G$  differentiable and  $I_1, I_2$  rapidly oscillating (periods  $t_1, t_2 \ll$  model time scale  $\Theta$ ). Then we may integrate by parts and drop terms of higher order in  $t_{1,2}/\Theta$ . With  $G(t, -\infty) = 0$  (7), and  $I_{1,2} = \bar{I} + \bar{I} \sum (4/\pi \ell) \sin 2\pi \ell t / t_{1,2}$  ( $\ell = 1, 3, 5, \dots$ ) for the analog of Fig. 1, we thereby reduce Eq. 4 to

$$\text{transient } (t > 0) \approx G(t, 0) \cdot [t_2 - t_1] \cdot \frac{1}{4} \bar{I} \quad (5)$$

with relative error  $\sim (t_{1,2}/\Theta)^2$ . This generalizes readily to  $G(t, 0) \cdot [m_2 t_2 - m_1 t_1] \cdot \bar{I} \sum (c_\ell / 2\pi \ell)$  for any  $I_{1,2}$  that are periodic and odd, differing only in period and perhaps modulation ( $m_{1,2}$ ) and with Fourier sine coefficients  $c_\ell$ . Thus abrupt changes in modulation or in period give similar effects. Note that Levinson's (5) pure sinusoids correspond to  $\sum (c_\ell / 2\pi \ell) = 1/2\pi$  and the special cases either  $m_1 = 0$  or  $m_2 = 0$ .

The transient Eq. 5 separates into a model factor  $G(t > 0, 0)$  and a stimulus factor  $\propto [t_2 - t_1]$ . If visibility corresponded solely to the size of the model transient, this would imply threshold curves  $t_1 \approx t_2 \pm$  a constant for any linear model, with only the constant dependent on specifics—which is the general trend observed (1). We defer numerical studies and consider now only the sign of the transient.

The polarity criterion follows at once from Eqs. 5 and 1: a model to be consistent with the polarity observations requires

$$G(t > 0, t' = 0) \text{ predominantly } < 0 \quad (6)$$

by whatever detection scheme the model assumes, that is, an acceptable model must have impulse response  $G$  detected as negative. This does not say the response to a finite pulse is negative, for that depends on  $\int G$ , including any singularities of  $G$  at  $t = t' = 0$  which are excluded in Eq. 6. Indeed the model had better give positive response to a step or a long "flash." Hence, Eq. 6 is a serious restriction.

The general power and facility of this polarity criterion is reflected in the fact that the great majority of proposed models are not immediately compatible

with it (8). A few examples must suffice here, selected for ease of illustration only and with no space to do justice to their merits in other respects. Perhaps most familiar are the "deLange models" [ $n$ -stage integrators, see (5)] for which  $G(t, t') = G_n(t - t')$  where  $G_n(t) = S(t) \exp(-t/\theta) (t/\theta)^{n-1} / (n-1)! \theta$ . This is always positive, so that Eq. 6 absolutely excludes a pure deLange model. The broader class of "deLange-Kelly models," which include also differentiations, have  $G(t, t')$  a linear combination of the above  $G_n$ 's and, as indicated earlier (4), only one is easily reconciled with Eq. 6. An example of the entirely different class of "Ives (diffusion) models" is Veringa's (8) for which the  $G$  (his  $R_\delta$ ) is positive and cannot be reconciled with the criterion Eq. 6. Finally, a nonlinear example is the nicely posed model of Sperling and Sondhi (8) which, on the basis of its linear limit and assumed detector, has  $G$  (their figure 7) unacceptable by our criterion.

Now consider the flash paradox. To resolve it in a linear model, the superposition principle requires that a brief input by itself give response detected as opposite in sign to the input. Previously (4), we found a simple amplitude-duration detector,—added to the allowed deLange-Kelly model in order to preserve steep flanks in "deLange curves"—also accomplishes this. Here we show it does the same for any model satisfying, as it ought, Eq. 6. Thus, for a rectangular input  $I = I_0$  for  $0 \leq t \leq \tau$  and  $I_0 = 0$  otherwise, Eq. 2 gives  $R(t) = I_0 \int_0^\tau G(t, t') dt'$ . Now if  $\tau$  is less than a duration threshold  $\Delta t$ , say, the initial response by itself is not detected, but only that at  $t > \Delta t > \tau$ . Then  $t > \tau \cong t'$  in  $\int_0^\tau G$ , so singularities again are excluded, and by parts

$$R(t > \tau) \approx G(t, 0) \cdot \tau \cdot I_0 \quad (7)$$

with relative error  $\sim \tau/\Theta$ . Hence, by Eq. 6, this detected response is opposite in sign to  $I_0$ , as desired. Further, superposing Eqs. 7 and 5, we see that their forms permit complete cancellation (5) for  $\tau \approx \frac{1}{4} [t_1 - t_2] \cdot (\bar{I}/I_0)$ .

We return finally to the eye. If superposition remains valid even very roughly, then also in the perception of brief flashes a nonconservation of polarity must somehow occur. However, if in reality polarity is conserved, the paradox deepens. In any event, the danger in interpreting observations on an assumption of polarity conservation (5), though in accord with most models, is pointed up by the flash paradox. Con-

versely, it is striking that direct perception gives so selective a test for models as the polarity criterion, Eq. 6.

J. F. BIRD

G. H. MOWBRAY

Applied Physics Laboratory,  
Johns Hopkins University,  
Silver Spring, Maryland 20910

#### References and Notes

1. D. M. Forsyth and C. R. Brown, *Science* **134**, 612 (1961); *ibid.* **135**, 794 (1962).
2. C. R. Brown and D. M. Forsyth, *ibid.* **129**, 390 (1959); L. Matin, *ibid.* **136**, 983 (1962).
3. T. K. Sen, *J. Opt. Soc. Amer.* **54**, 386 (1964).
4. G. H. Mowbray and J. F. Bird, *Acta Psychol.* **30**, 84 (1969); *Donders' Centenary Symposium* (Eindhoven, Netherlands, July 1968).
5. J. Z. Levinson, *Science* **160**, 21 (1968). The stimulus he used was essentially the fundamental sinusoidal component of Fig. 1, but with zero modulation for either the first or second train (that is,  $t_1 = 0$  or  $t_2 = 0$  in Eq. 1, for any but infinitely fast vision). He states the transients look alike near threshold, and to try to distinguish he inserts flashes with results as indicated above. He implies this determines a polarity for the transients which would be opposite to our experience (Eq. 1), and of course no paradox then appears. However, it is inappropriate to measure the transients this way, because one does not know how the combined response is related to the separate responses; and even if simple linearity (additive responses) be granted, it is not necessarily valid to equate subjective and objective polarities. If instead we accept the polarity given in Eq. 1, and these flash effects, the paradox remains.
6. H. deLange, *J. Opt. Soc. Amer.* **44**, 380 (1954).
7. C. Lanczos, *Linear Differential Operators* (Van Nostrand, London, 1961), pp. 244 and 330.
8. In preparation by the authors. Models considered include: H. E. Ives, *J. Opt. Soc. Amer.* **6**, 343 (1922); P. W. Cobb, *ibid.* **24**, 91 (1934); F. T. Veringa, *Kon. Ned. Akad. Wetensch.* **B64**, 413 (1961); H. deLange, *J. Opt. Soc. Amer.* **51**, 415 (1961); D. H. Kelly, *ibid.*, p. 747; J. Levinson and L. D. Harmon, *Kybernetik* **1**, 107 (1961); J. Levinson, *J. Opt. Soc. Amer.* **56**, 95 (1966); L. Matin, *ibid.* **58**, 404 (1968); G. Sperling and M. M. Sondhi, *ibid.*, p. 1133; and related models for nonhuman eyes: M. G. F. Fuortes and A. L. Hodgkin, *J. Physiol.* **172**, 239 (1964); R. D. DeVoe, *J. Gen. Physiol.* **50**, 1993 (1967).
9. Supported in part by PHS grant NB 07226-01. 15 January 1969; revised 13 May 1969

#### Carbon: Observations on the New Allotropic Form

Abstract. *The recently characterized "white" allotropic form of carbon has been produced at high temperature and low pressure during graphite sublimation. Under free-vaporization conditions above  $\sim 2550^\circ\text{K}$ , the white carbon forms as small transparent crystals on the edges of the basal planes of graphite. The interplanar spacings of this material are identical to those of a carbon form noted in graphitic gneiss from the Ries Crater.*

The new allotropic form of carbon has been produced during the sublimation of pyrolytic graphite (1, 2). Small bars of pyrolytic graphite (2 by 3 by 40 mm) were heated resistively to tem-

Table 1. Electron diffraction data for white layer on pyrolytic graphite.

Observed $d$ (Å)	Calculated <sup>a</sup> $d$ (Å)	Difference (Å)	$hkl$
4.457	4.465	-0.008	11.0
2.571	2.577	-0.006	30.0
2.234	2.232	+0.002	22.0
1.681	1.688	-0.007	14.0
1.496	1.488	+0.008	33.0
1.283	1.288	-0.005	60.0
1.238	1.238	0.000	52.0
1.118	1.116	+0.002	44.0
1.030	1.024	+0.006	17.0
0.975	0.974	+0.001	63.0
0.899	0.893	+0.006	55.0
0.865	0.859	+0.006	90.0
0.833	0.844	-0.011	82.0
0.802	0.802	0.000	47.0
0.747	0.744	+0.003	66.0
0.738	0.734	+0.004	10 1.0
0.719	0.715	+0.004	39.0
0.675	0.681	-0.006	58.0
0.645	0.644	+0.001	12 0.0
0.636	0.638	-0.002	77.0

\* Calculation based on  $a = 8.948 \text{ \AA}$  (1).

peratures between 2700° and 3000°K in an atmosphere of argon at a pressure of  $10^{-4}$  torr. Specimens were oriented so that electrical contact was made on the edges of the graphite basal planes. After 15 to 20 seconds of heating the rods showed a silvery white coating in the region of maximum temperature (Fig. 1A). The white coating did not form below about 2550°K. The experiments were carried out under conditions of free vaporization; hence, the gas pressure immediately above the graphite could probably not have exceeded a few microns.

The sublimation-etched pyrolytic graphite bar was examined with scanning electron microscope (Fig. 1, B and C), electron microprobe, and electron diffraction (3). Clearly, there is a marked difference in surface morphology between the white area and the surrounding graphite. The white area in the scanning electron micrograph con-

sists of dendritic formations about  $0.5 \mu$  in diameter and 5 to  $10 \mu$  long. Presumably, they were formed by migration of carbon atoms, since the free-vaporization conditions would not favor condensation on the hottest region of the bar. Even though white carbon was most conspicuous on basal plane edges, it also formed on basal plane surfaces but was most evident on the basal plane edges forming the walls of etch pits in the basal planes of the pyrolytic graphite. The graphite (Fig. 1C) shows the characteristic laminate form of the basal plane edges with layers about  $0.1 \mu$  thick. An electron microprobe analysis was made at several locations on the white area and on the adjoining black area. The microprobe would detect all elements from boron to uranium. Aside from carbon, only silicon (0 to 2.5 percent by weight) was detected. The largest concentration of silicon occurred in the white area, but its source is unknown.

An electron diffraction pattern of the white coating was obtained by directing the electron beam tangent to the white area (Fig. 1D). The rings correspond to reflections from finely crystalline turbostratic graphite which underlies the white material, and were used to calibrate the pattern ( $c_0 = 6.84 \text{ \AA}$ ). The hexagonal pattern of spots shows that the white dendrites are single crystals of hexagonal symmetry, and that the electron beam was parallel to the  $c$  axis. Moreover, all the dendrites must have the same crystallographic orientation because the diameter of the electron beam was much larger than the width of a single dendrite. We thus appear to be dealing with single crystal material of unusual habit. Measurement of the diffraction pattern yielded the  $d$  values and corresponding indices given in Table 1. The average value obtained for the hexagonal cell dimension  $a_0$  was  $8.939 \pm 0.035 \text{ \AA}$  mean deviation. This is within experimental error of the reported value,  $a_0 = 8.948 \pm 0.009 \text{ \AA}$  (1). Also the indices given in Table 1 satisfy the rhombohedral

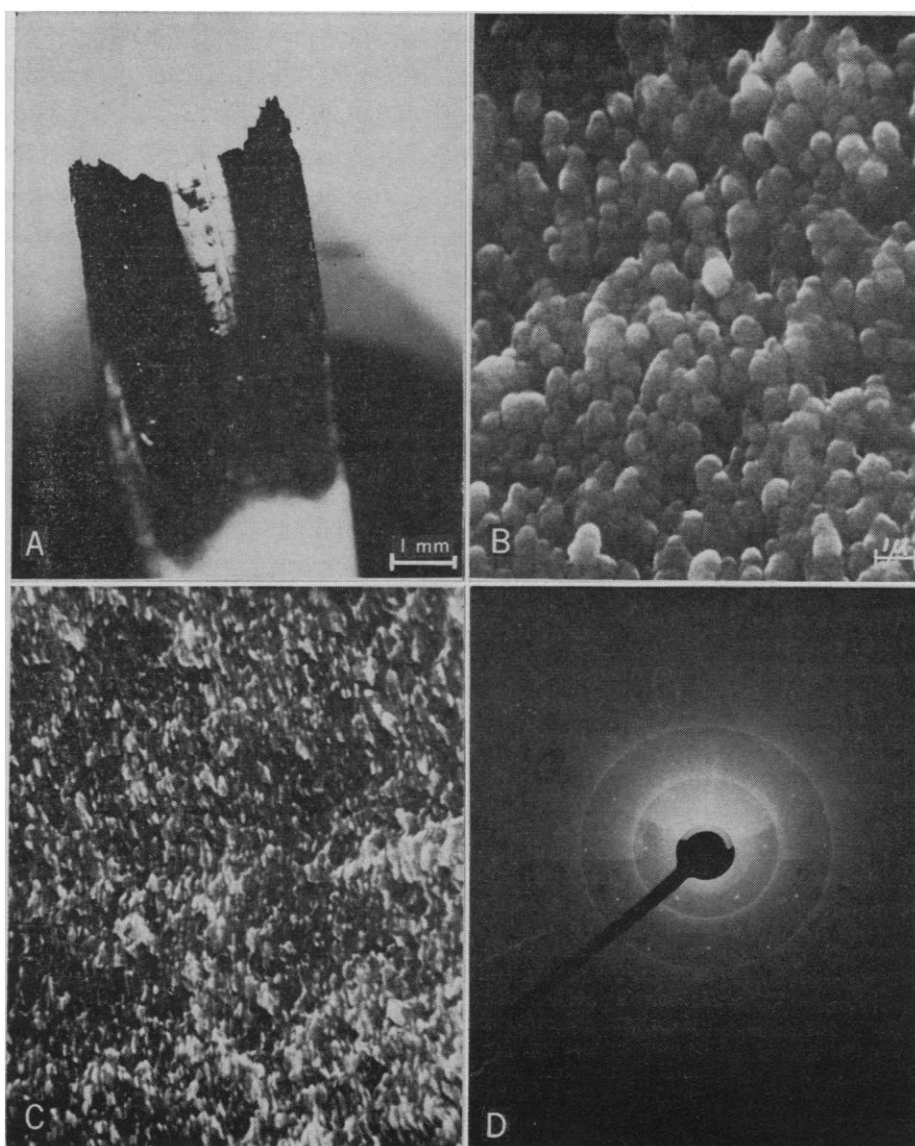


Fig. 1. (A) Direct photograph of half of the pyrolytic graphite bar showing appearance and location of the white carbon. (B) Scanning electron micrograph of the white area (approximately  $\times 3450$ ). The grainy appearance is due to unresolved surface structure, not to photographic procedures. (C) Similar micrograph at the same magnification of the adjacent graphite. (D) Electron diffraction pattern showing rings due to turbostratic graphite and spots due to white carbon.

condition, in that  $-h + k + l = 3n$ . Since the electron beam was parallel to the  $c$  axis, only  $l = 0$  reflections were obtained, and only the  $a_0$  parameter could be determined. Nevertheless, the agreement on the  $a_0$  parameter and the silvery white appearance of the material leave little doubt that the coating on the graphite is the same substance as that found in the graphitic gneiss from the Ries Crater (1). However, conditions of formation here indicate that it is very unlikely that this white allotropic form of carbon is a high-pressure form as was originally inferred. Indeed the conditions under which we produced the new form of carbon were low pressure and high temperature.

There were reflections in the diffraction pattern that did not fit the hexagonal array. Some of these were measured and were found to form a rectangular pattern and the  $d$  values correspond to  $\alpha$  SiC form I (4). This indicates that the electron beam was normal to an  $a$  axis of SiC to give only  $k = 0$  reflections and implies that the SiC crystals had a fixed orientation to either the white carbon crystals or the graphite basal planes. The white carbon contained about five times as much silicon as the natural material described by El Goresy and Donnay (1). This had no measurable effect on the  $a_0$  parameter; hence, it is unlikely that the silicon is directly involved in the white carbon phase. Silicon may act as a flux for the formation of the white carbon; however, additional experiments showed that white carbon can be just as easily synthesized in a silicon-free system.

The white carbon coating is a transparent birefringent material; therefore, its white appearance is due to light scattered by the large number of surfaces. Also, the extinction behavior agreed with the observation that all the dendrites had the same crystallographic orientation, and with the implication that they grew perpendicular to the edges of the basal planes with an  $a$  axis parallel to the planes. Unfortunately, no index of refraction data could be obtained because the crystals were much too small.

In an article entitled "Dendrites of graphite" (5) four figures show dendritic growth identical to that which we observe in the new phase of carbon. It thus appears likely that this new phase, which often appears as a transparent coating on graphitic crystals, may have been missed repeatedly in the past.

*Note added in proof:* Twenty-three additional  $d$  values which were ob-

tained from several small randomly oriented white carbon crystals were used to calculate the unit cell dimensions:  $a_0 = 8.945 \pm 0.007$  Å,  $c_0 = 14.071 \pm 0.011$  Å.

A. GREENVILLE WHITTAKER  
P. L. KINTNER

Materials Sciences Laboratory,  
Aerospace Corporation,  
El Segundo, California

#### References and Notes

1. A. El Goresy and G. Donnay, *Science* **161**, 363 (1968).
2. A. G. Whittaker and P. Kintner, *Carbon*, in press.
3. The scanning electron microscope was a Cambridge Stereoscan Mark 2 operated at 20 kv with a spot diameter of  $\sim 100$  Å; the

electron microprobe was an Applied Research Laboratories model EMX with a beam diameter of  $\sim 0.5$   $\mu$  at  $\sim 4$   $\mu$  penetration; the electron microscope used for the electron diffraction work was a Jeolco model 5 G with a beam diameter of  $\sim 2$   $\mu$  and a beam energy of 80 kv.

4. N. W. Thibault, *Amer. Mineral.* **29**, 327 (1944).
5. I. Nakoda and Y. Tamai, in SM-68016 Applications of the Japan Electron Optics Laboratory Scanning Electron Microscope (Jeolco, Ltd., Medford, Massachusetts), p. 11.
6. We thank H. Parish and J. Dancy (Naval Weapons Center, China Lake, California) for scanning electron microscopy and electron diffraction work, respectively; G. M. Wolten and J. H. Richardson (Aerospace Corporation) for assistance in interpretation of the electron diffraction pattern and photography, respectively; and J. Ogren and R. Commingham (Autonetics, North American Rockwell Corporation, Anaheim, California) for electron microprobe analysis.

28 May 1969

## Enstatite: Disorder Produced by a Megabar Shock Event

**Abstract.** Shocked Bamle enstatite partly transforms to disordered enstatite. Debye-Scherrer patterns of some shocked material are almost identical to those of disordered enstatite from portions of various enstatite achondrites. No disordered single crystals have been found.

Disordered enstatite (1), which was first found in 1963 (2) in Cumberland Falls and Norton County achondrites, was subsequently found in all the enstatite achondrites except those from Shallowater (3). The presence of disordered enstatite was also noted in five enstatite chondrites, 20 ordinary chondrites, and in synthetic samples cooled fairly rapidly from 2800°C (4). Since the enstatite achondrites, except Shallowater, are highly brecciated, one possible origin of the disordered enstatite is shock deformation. Samples of enstatite from Bamle, Norway, shocked at 150 to 200 and 400 to 450 kb did not show evidence of disordered

enstatite (4). We now report the observation of disordered enstatite in samples shocked to pressures of approximately 1 Mb.

Disks of Bamle enstatite,  $\sim 19$  mm in diameter by 2.5 mm thick, were fitted into stainless steel sample capsules, which in turn were fitted into holes in a steel block surrounded by steel spall plates. The capsule assemblies were impacted by a stainless steel disk (3 mm thick) which had been explosively accelerated to a velocity of 3.6 to 3.7 km/sec. Peak shock pressures in the samples were in the range of 0.9 to 1.0 Mb, and the duration of the pressure pulse was less than 1  $\mu$ sec.

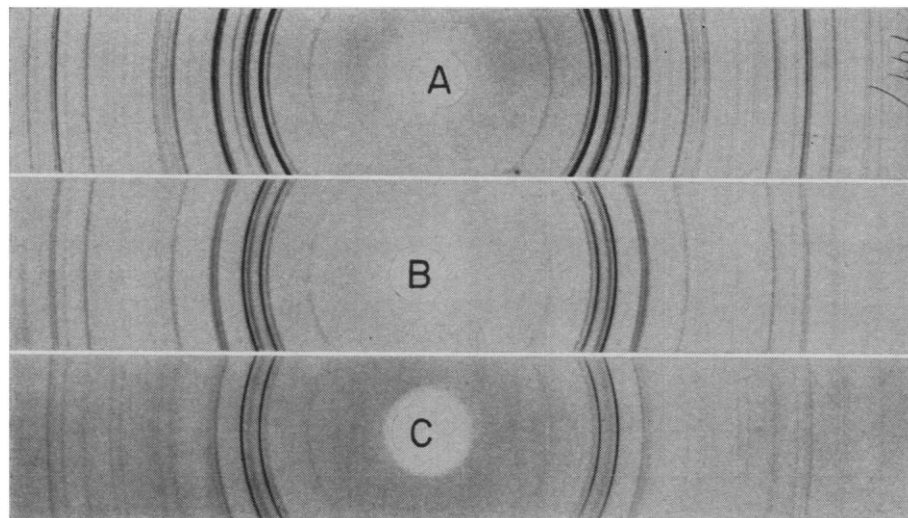


Fig. 1. Debye-Scherrer photographs of ordered enstatite from Khor Temiki enstatite achondrite (A); disordered enstatite from Aubres enstatite achondrite (B); and disordered enstatite from Bamle enstatite shocked at 1 Mb (C).